Check for updates

Journal of Morphology

WILEY

JOURNAL OF morphology

RESEARCH ARTICLE

Feeding in the Korean Plethodontid Salamander *Karsenia* and Its Evolutionary Implications

Yu Zeng[1] | Jiho Park[2,3] | Yucheol Shin[4,5] | Daesik Park[2] | Stephen M. Deban[1]

[1]Department of Integrative Biology, University of South Florida, Tampa, Florida, USA | [2]Department of Science Education, College of Education, Kangwon National University, Chuncheon, Republic of Korea | [3]Interdisciplinary Program in Earth Environmental System Science & Engineering, College of Natural Sciences, Kangwon National University, Chuncheon, Republic of Korea | [4]Department of Herpetology, Division of Vertebrate Zoology, American Museum of Natural History, 200 Central Park West, New York, New York, USA | [5]Richard Gilder Graduate School, American Museum of Natural History, 200 Central Park West, New York, New York, USA

Correspondence: Yu Zeng (yuzeng@usf.edu)

Received: 30 July 2026 | **Revised:** 5 October 2026 | **Accepted:** 3 November 2026

Keywords: feeding kinematics | hyobranchial apparatus | predation

ABSTRACT

The lungless salamanders (Plethodontidae) exhibit remarkable diversity in tongue feeding mechanisms, ranging from short-range protrusion to some of the longest and fastest projectile tongues among amphibians. However, the evolutionary pattern of tongue mechanisms within plethodontids remains incompletely resolved because the feeding behavior and tongue kinematics of *Karsenia koreana*, the only Asian plethodontid, have not been documented. Here, we report the first description of tongue morphology and function during feeding in *Karsenia* based on high-speed videography and dissection. We found that adult *Karsenia* captured prey from a horizontal distance of approximately 4 mm from the tip of the lower jaw, equivalent to about 10% of snout-to-vent length. During feeding, the tongue protruded at a mean speed of 0.13 m/s, while the tongue pad rotated forward at a mean angular speed of approximately 5790°/s. Both tongue protrusion and tongue pad rotation decelerated toward maximum reach. These results indicate that *Karsenia* uses a protrusive tongue mechanism, which is consistent with direct muscular actuation. Phylogenetic mapping suggests that ballistic tongue projection evolved twice within Plethodontidae. Two Old World plethodontid lineages with contrasting tongue mechanisms—a protrusive tongue in *Karsenia* and an extreme projectile tongue in *Speleomantes*—is consistent with the hypothesis that plethodontids were once more broadly distributed and functionally diverse in Eurasia. The survival of these two lineages may reflect historical biogeographic contingency.

1 | Introduction

With the ability to reach and capture distant prey, protrusive tongues are important adaptations for terrestrial life. The lungless salamanders (Family Plethodontidae) have evolved diverse tongue types that perform at various reaches and speeds, ranging from short-reach protrusive tongues (e.g., *Plethodon*) to long-reach projectile tongues (e.g., *Hydromantes*) (Wake and Deban 2000).

The ancestral tongue type of plethodontids is a protrusive tongue. The tongue protrudes from the mouth by the contracting subarcualis rectus (SAR) muscles pulling on the epibranchial cartilages of the tongue skeleton. While protrusive tongues are found in some extant plethodontid lineages (e.g., *Plethodon* and *Desmognathus*), selection for faster, farther, and energetically more efficient tongue projection has driven the transition from protrusive to ballistic tongues (Zeng and Deban 2026). Such specialization involves a muscle-skeleton disassociation and a formation of sliding-based linear actuation between the SAR muscles and the epibranchial (EB) cartilages (Lombard and Wake 1977; Wake and Deban 2000; Deban et al. 2020; Zeng et al. 2025). The innovation of ballistic projection likely has

All rights reserved, including rights for text and data mining and training of artificial intelligence technologies or similar technologies.

© 2026 Wiley Periodicals LLC.

promoted the diversification of plethodontids, especially the subfamily Hemidactyliinae, in the New World.

The presence of the genioglossus muscles (GG), a pair of muscles that connect the mandible to the distal end of the tongue, is also a characteristic feature of protrusive tongues. In protrusive tongues among salamanders, the genioglossus muscles function to move the tongue forward during protrusion and also involved in tongue pad rotation, as shown in plethodontids and other families, such as *Ambystoma* (Wake and Deban 2000). Besides the GG muscles, the glossal ligaments (GL) can also transmit the folding action of the hyobranchial skeleton to a pulling force that assists in tongue pad rotation (Lombard and Wake 1977).

In plethodontids, GG muscles are present in protrusive tongues and some ballistic tongues (i.e., "attached ballistic tongues", as in *Ensatina* and *Batrachoseps*). Some ballistic tongues have complete loss of GG (i.e., "free ballistic tongues", as in *Bolitoglossa*), and the tongues are projected free of any attachment to the lower jaw (Lombard and Wake 1986). These three classes of tongue mode encompass much of the functional variation within Plethodontidae, particularly in the subfamily Plethodontinae, and their distribution across lineages reflect a pattern of homoplasy (Lombard and Wake 1986; Wake 1991).

The majority of plethodontids live in the New World, with two exceptions: the European cave salamanders (*Speleomantes* spp.) and the Korean Crevice Salamander (*Karsenia koreana*; Min et al. 2005). In particular, *Karsenia* is a monotypic genus that has only been documented from the woodlands of the Korean Peninsula. Both *Karsenia* and *Speleomantes* are in the subfamily Plethodontinae but likely resulted from two independent dispersals via Beringia from western North America some 60 million years ago (Vieites et al. 2007; Shen et al. 2016; Stewart and Wiens 2025). Unlike *Speleomantes* and its sister clade *Hydromantes*, whose tongue function has been well studied (Deban et al. 1997, 2007), the feeding morphology and kinematics of *Karsenia* have remained undocumented, creating a gap in our understanding of tongue evolution in plethodontids.

Previous examination of *Karsenia* based on preserved specimens suggested a protrusive tongue, attributed to morphological similarity with sister taxa (e.g., *Plethodon*), such as round tongue pad, the lack of posterior flap of tongue pad and relatively short epibranchial cartilages (Min et al. 2005; Buckley et al. 2010). Nevertheless, the available data did not fully exclude a possibility that *Karsenia* is a cryptic ballistic-tongued species, like *Ensatina* (Deban and Scales 2016), especially given the variation of tongue designs in plethodontids, shared presence of GG muscles between protrusive and some ballistic tongues, and the lack of data on the myofiber connection between SAR muscles and EB. Therefore, direct observation of how *Karsenia* feeds and the morphology of its feeding apparatus are critical.

Here, we examine the tongue feeding mechanism of *Karsenia*. First, we characterize tongue feeding behavior and kinematics based on high-speed videography. The speed of tongue launch can be used to examine whether the tongue is muscle-powered or ballistically actuated based on a threshold speed of approximately 1 m/s (Zeng et al. 2025). Second, we document the morphology of the hyobranchial system in fresh specimens. Third, we compare tongue feeding capability of *Karsenia* with those of other species from a published data set (Zeng et al. 2025). Lastly, we interpret tongue mechanism evolution of plethodontid salamanders in a phylogenetic context. Our results help to clarify the evolutionary pattern of tongue mechanisms in plethodontids and enrich the understanding of historical patterns in both the distribution and tongue functional diversity in salamanders.

2 | Materials and Methods

On May 16, 2026, we collected ten *K. koreana* from Mt. Jangtae, Daejeon Metropolitan City, Republic of Korea. The field survey was conducted by flipping fallen logs, leaf litter, and rocks along a stream valley. All flipped objects were returned to their original positions to minimize disturbance to the microhabitat. The collected salamanders, including eight adults and two juveniles, were transported to the Laboratory of Herpetology at Kangwon National University in a portable cooler with ice packs to minimize heat stress. Salamander maturity was determined based on the SVL range from literature (Min et al. 2005), but salamander sex was not identified due to very few intersexual differences in external morphology (see Supplemental Data 1 for details).

After transport to the lab, we individually housed the salamanders in plastic cups with ventilated lids approximately 10 cm in diameter and 5 cm in height. Individuals were numbered and photographed in dorsal view while lying on a flat surface. We measured snout-to-vent length (SVL) from digital images taken with a scale bar using ImageJ (Rueden et al. 2017), and measured body mass (m) using an electronic balance (K17, CAS Corporation, Yangju-si, Republic of Korea).

To examine the anatomy of the hyobranchial system, we dissected two adult individuals (No. 5, m = 1.8 g, SVL = 42.5 mm; No. 7, m = 3.1 g, SVL = 49.4 mm; see below). Specimens were deposited at the Laboratory of Herpetology at Kangwon National University. After the experiments, the remaining eight individuals were released at the original collection locality on May 23, 2026. The field and experimental protocols were reviewed and approved by the Institutional Animal Care and Use Committee of Kangwon National University (KW-260329-6), and specimen collection was performed under a research permit issued by the Daejeon Metropolitan City Seo-gu Office (permit No. 2026-1).

2.1 | Feeding Trials and High-Speed Videography

Feeding observations and recordings were conducted in the basement of the College of Education building at Kangwon National University, with dim light from cellar windows. The room temperature was maintained approximately 20°C, similar to the temperature of their natural microhabitat. The salamanders were kept in the same room except for the first night (May 16), when they were kept in a refrigerator at 15°C. Feeding sessions started on 10 a.m., May 17, 2026, with acclimation time approximately 18 h, and lasted until 2 p.m., May 19, 2026.

10974687, 2026, 12, Downloaded from https://onlinelibrary.wiley.com/doi/10.1002/jmor.70195 by Yucheol Shin - American Museum Of Natural , Wiley Online Library on [25/11/2026]. See the Terms and Conditions (https://onlinelibrary.wiley.com/terms-and-conditions) on Wiley Online Library for rules of use; OA articles are governed by the applicable Creative Commons License

The experimental arena consisted of a brick ($10 \times 20 \times 5$ cm) covered with wet tissue paper and placed inside a larger storage box positioned on its side. Light was blocked from all directions except the side facing the camera. Additional illumination was provided by infrared LED arrays.

Commercially obtained green bottle fly maggots (*Lucilia sericata*) were used as prey (length, 7–9 mm; mass, ~60 mg). Salamanders were placed individually in the imaging arena and provided 10–30 min per feeding session. Feeding sessions were rotated between eight adults. During experiments, we gently sprayed the salamanders and arena with aged tap water several times to prevent desiccation.

As no information was available on feeding behavior of *Karsenia*, we initially tested their response to prey placed at various distances in the arena and allowed them to explore and feed. After initial trials, we used wet brown paper towel, which provided a visual contrast against the pale-colored prey, and placed one to five prey 5–50 mm in front of the salamander.

Feeding events were recorded using a high-speed video camera (Edgertronic SC1; Sanstreak Co. San Jose, CA, USA) at 1000 frames per second in post-trigger mode, with the lens (Nikon AF Nikkor 50 mm f/1.8D) about 40 cm away from the arena. The salamander's behavior was monitored on a computer screen and captured once feeding was observed. Once prey was successfully captured, the salamanders were allowed to feed on it without restriction.

2.2 | Tongue Kinematics

Tongue performance was compared with that of a *Plethodon metcalfi* feeding on a termite, imaged in lateral view. Protrusion and retraction periods were obtained from all eight recorded trials, from which gape and tongue movements were clearly visible. The protrusion period was calculated as the duration between (1) the onset of mouth opening and (2) the tongue tip reaching its maximum extent. The retraction period was calculated as the duration between (1) the onset of tongue retraction and (2) the retracted prey stopped at the mandibular joint, immediately followed by mouth closing.

For the kinematics of tongue protrusion and tongue pad rotation, we used two trials (one from each of individual No. 2 and No. 8) in which the salamanders were imaged in lateral view. We tracked landmarks from lateral images using DLTdv8 (Hedrick 2008). A total of five landmarks were tracked: (1) the anterior margin of the mandible and the jaw joint, which were used to calculate jaw orientation and movement relative to the global coordinate system; (2) the approximate distal end of the basibranchial (BB), which represented the anterior position of the tongue skeleton; and (3) the anterior and posterior ends of the tongue pad, which were used to describe tongue pad orientation. In particular, the anterior end of the tongue pad was approximated by the basal position of the radial cartilages (Figure 2A).

Using custom R scripts (R Core Team 2023), we reconstructed the trajectories of the distal end of the BB and the two tongue pad landmarks. Tongue kinematics was described with respect to a coordinate system centered at the anterodorsal tip of the lower jaw, with x-axis parallel to the vector extending from the tip of the lower jaw to the mandibular joint. Tongue pad orientation (θ) was represented by a vector pointing from the anterior edge to the posterior edge of the tongue pad.

We then calculated the translational speed of the distal end of the BB (u) and the angular speed of the tongue pad (ω). Reach ($d_{[\max]}$) was calculated as the maximum distance between the posterior end of the tongue pad (i.e., the farthest point on the tongue pad from the animal) and the anterior margin of the mandible. To examine the coupling between tongue protrusion and tongue pad rotation, we extracted the locations of the distal end of BB when the peaks of u and ω happened and then normalized them by the maximum reach of the distal end of the BB.

For the two feeding trials, the mean protrusion speed ($\bar{u}$) and mean tongue pad rotation speed ($\bar{\omega}$) were summarized based on the observed protrusion period (T_{prot}), which was calculated as the time interval between the start of BB protrusion and the BB reaching the maximum excursion.

2.3 | Anatomical Examination

The salamanders were euthanized by immersion in a buffered MS-222 solution (500 mg/L) for 60 min before dissection. Photographs were taken using an iPhone SE (Apple Inc., California, USA) while the specimens were immersed in saline solution. Muscle identification followed previous descriptions (Lombard and Wake 1977).

Fully euthanized salamanders were positioned ventral side up. Saline-moistened tissue paper was used to keep the body surface moist during dissection. First, we used forceps to manipulate the tongue and examine the connection between the tongue pad and the lower jaw. We then opened the pharyngeal region and removed the overlying skin and superficial muscles, including the geniohyoideus medialis, to expose the hyobranchial skeleton. Next, we removed the skin from the right lateral side of the neck to expose the subarcualis rectus (SAR) muscle and record its configuration before and after the tongue was pulled to its maximum extent with forceps. The abdominal skin was then reflected laterally to expose the two rectus cervicis profundus (RCP) muscles.

We next documented the morphology of the tongue skeleton in relaxed and folded (protruded) states. In one specimen (No. 5), the skin and soft tissues surrounding the tongue stalk were removed to fully expose the tongue skeleton, including the basibranchial (BB) and glossal ligaments (GL). The isolated tongue skeleton was placed ventral side up and gently compressed with forceps near the CB-EB joints to assess its recovery after mechanical deformation.

In the other specimen (No. 7), we first transected the RCP muscles from the ventral side and then pulled the tongue outward to expose the configuration of the folded tongue skeleton. The entire tongue stalk was then extended, and the SAR insertion at the ceratohyal was cut to isolate the tongue stalk in

10974687, 2026, 12, Downloaded from https://onlinelibrary.wiley.com/doi/10.1002/jmor.70195 by Yucheol Shin - American Museum Of Natural , Wiley Online Library on [25/11/2026]. See the Terms and Conditions (https://onlinelibrary.wiley.com/terms-and-conditions) on Wiley Online Library for rules of use; OA articles are governed by the applicable Creative Commons License

its folded state. We documented the configuration of the folded tongue skeleton, including the taut glossal ligaments and tongue pad. Finally, the remaining soft tissues were removed to expose the radial cartilages.

2.4 | Comparative Analysis

First, we compared tongue feeding performance among *Karsenia*, other plethodontids, and non-plethodontid salamanders. Genus-level mean values were obtained from the literature (Zeng et al. 2025). Prey used in these studies included small flies, maggots, and termites, which were generally small relative to the salamanders and could be swallowed whole. For *Karsenia*, mass-specific power (3.9 W/kg) was approximated by assuming an acceleration period of 10 ms, comparable to the time scale of tongue protrusion, and an acceleration of approximately 19 m/s^2.

We then updated the inferred evolutionary pattern of tongue mechanisms in plethodontids. First, we used a recent phylogeny (Stewart and Wiens 2025) and mapped *Karsenia* and other plethodontid taxa to infer the origins of ballistic projection under a parsimony criterion. Tongue mechanism states (ballistic or protrusive) at the genus level were obtained from the literature (see Deban et al. 2020). A schematic visualization of geographic distributions was developed using distribution data for terrestrial salamander families, including Ambystomatidae, Hynobiidae, Salamandridae, Rhyacotritonidae, and Dicamptodontidae, obtained from AmphibiaWeb (AmphibiaWeb 2026).

3 | Results

We successfully recorded eight feeding trials from two adults, with two from No. 2 ($m = 2.2$ g, SVL = 43.3 mm) and six from No. 8 ($m = 3.1$ g, SVL = 45.1 mm). All feeding trials were recorded on the first day (May 17, 2026) after the salamander were transported to the laboratory. No failed tongue strikes or repeated attempts were observed.

Tongue protrusion speed averaged 0.13 m/s, more than an order of magnitude lower than the ~1.5 m/s speeds associated with ballistic launch (Zeng et al. 2025). These results indicate that *Karsenia* uses a muscle-powered protrusive tongue. Below, we first describe the feeding sequence qualitatively, followed by detailed kinematics. We then present further details of the configuration of the tongue skeleton and addressed Karsenia's tongue capability within a comparative context.

3.1 | Feeding Behavior

The feeding sequence was similar to that of other terrestrial, protrusive-tongued salamanders and consisted of three main phases: (1) preparation, (2) capture, and (3) deglutition. In general, the salamanders first detected the prey, a light-colored maggot presented against a dark background, then pitched down and oriented the snout toward the prey. Next, the tongue protruded, captured prey and retracted quickly, followed by swallowing of the prey (Movies 1 and 2).

High-speed videos revealed that the capture phase began with mouth opening, during which the tongue was already moving forward. As the tongue continued to protrude, the anterior portion of the tongue pad and the connective tissue between the tongue pad and mandible rolled ventrally. (Figure 1A–C). Simultaneously, the tongue pad rotated forward and formed a V shape in frontal view (Figure 1D). This bifurcated configuration of the tongue pad may have been observed previously in other species but, to our knowledge, has not been explicitly described or analyzed together with its rotational kinematics. As the tongue approached maximum reach, the initially dorsal surface of the tongue pad contacted and adhered to the prey.

After adhesion, the tongue stalk continued to move forward for a short distance before retraction began. During retraction, the tongue pad carried the prey and rotated in the opposite direction. Once the prey reached the buccopharyngeal region, the salamander closed its jaws and subsequently swallowed the prey. The overall feeding sequence was similar to that of other plethodontids with protrusive tongues (such as *Plethodon*; Figure 1B), although we did not observe a forward body lunge.

3.2 | Tongue Kinematics

Tongue movement was characterized from the displacement of the distal end of the basibranchial (BB) and the rotation of the tongue pad in two trials imaged in lateral view. The total duration of the feeding strike ranged from 30 to 50 ms (44 ± 6.6 ms; mean ± S.D., same below; $N = 2$ for individual No. 2; $N = 6$ for individual No. 8).

More detailed kinematics were only available from two feeding trials imaged in lateral view, one from each of imaged individuals (i.e., No. 2 and No. 8). The trajectory of the distal end of the BB was relatively straight and directed anteroventrally, forming a narrow out-and-back loop (Figure 2A,B). The protrusion distance of the distal end of the BB ranged from 2.2 to 3.6 mm (2.9 ± 1.0 mm; $N = 2$). Reach, measured from the posterior edge of the tongue pad, ranged from 3.7 to 4.6 mm (4.1 ± 0.7 mm; $N = 2$). Following the linear trajectory, tongue protrusion speed averaged 0.13 ± 0.05 m/s ($N = 2$). Tongue protrusion appeared to begin before mouth opening, as indicated by the high velocity at the beginning of the tracked sequence. The initial measured protrusion velocity was 0.19 ± 0.01 m/s and occurred when the distal end of the BB was near the tip of the lower jaw ($d' = 0.18 \pm 0.26$; Figure 2E). The distal end of the BB decelerated continuously as it approached maximum reach and accelerated in the opposite direction during retraction (Figure 2C). The mean acceleration during protrusion ($a = -5.4 \pm 0.7$ m/s^2; maximum value $a_{[max]} = -23.8 \pm 13.2$ m/s^2; $N = 2$) and that during retraction ($a = -8.1 \pm 1.9$ m/s^2; maximum value $a_{[max]} = -23.9 \pm 8.7$ m/s^2; $N = 2$) were comparable in magnitude.

Forward translation of the tongue stalk was coupled with rotation of the tongue pad. The pad rotated from an initial orientation of $\theta \approx 180°$ to ~100° (range 95°–101°) at first contact with the prey and reached a minimum angle of 45–72° later in the strike (Figure 2D). Of the two analyzed trials imaged in lateral view, the angular speed of tongue pad rotation averaged

10974687, 2026, 12, Downloaded from https://onlinelibrary.wiley.com/doi/10.1002/jmor.70195 by Yucheol Shin - American Museum Of Natural , Wiley Online Library on [25/11/2026]. See the Terms and Conditions (https://onlinelibrary.wiley.com/terms-and-conditions) on Wiley Online Library for rules of use; OA articles are governed by the applicable Creative Commons License

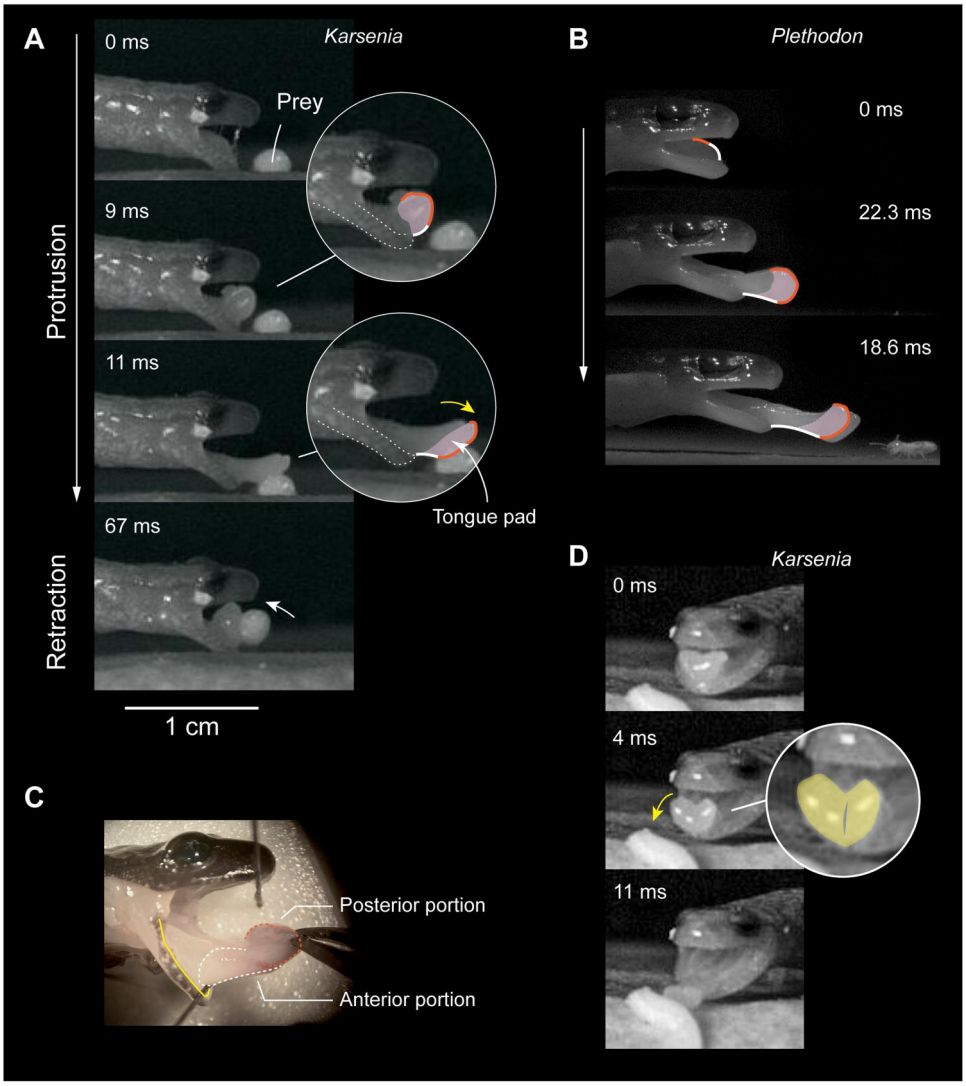


FIGURE 1 | Tongue feeding performance of *Karsenia*. (A) A full feeding sequence from tongue protrusion to retraction (individual No. 8). (B) Tongue protrusion in a *Plethodon metcalfi*. In (A) insets and (B), the tongue pad is highlighted in pink, with colored lines denoting the tongue pad surface (orange) and the tissue connection between the tongue pad and the lower jaw (white). (C) The tissue connection between tongue pad and the lower jaw on a fresh specimen (individual No. 7). (D) *Karsenia* tongue protrusion sequence in frontal view (individual No. 8). Inset highlights the V-shaped dorsal surface of tongue pad. See also Movies 1 and 2.

$5790° \pm 970$ °/s ($N = 2$). Peak angular acceleration occurred before the distal end of the BB passed the tip of the lower jaw ($d' = -0.21 \pm 0.29$). Correspondingly, peak angular velocity ($-12360° \pm 2060°$/s) was reached when the distal end of the BB was near the tip of the lower jaw ($d' \approx 0.06$).

3.3 | Hyobranchial Reconfiguration During Tongue Protrusion

We examined the configuration of the hyobranchial system in fresh specimens, focusing on reconfigurations associated with tongue protrusion. Externally, the subarcualis rectus (SAR) muscles were visible as a raised region in dorsal view and extended posterodorsally along the posterior margin of the skull (Figure 3A). The anterior portion of the tongue pad was connected to the anterior region of the mandible by the geniohyoglossus (GG) muscles (Figure 3B), a configuration similar to that of *Plethodon* (Lombard and Wake 1977). In addition, the rectus cervicis profundus (RCP) muscles originated from the pelvis and insert on the anterodorsal region of the basibranchial cartilage (Figure 3B–C).

The tongue pad rolled ventrally as the tongue skeleton protruded. At rest, the tongue pad was positioned near the center of the buccal floor. Gently pulling the tongue outward with forceps placed posterior to the tongue pad allowed the tongue stalk and associated elements to be examined in a protruded configuration (Figure 3D). The posterior end of the SAR muscles moved together with the posterior tip of the epibranchial (EB) cartilages as both shifted anteriorly. This coordinated displacement was consistent with a tissue connection between the SAR and EB, a characteristic of protrusive tongues (Figure 3A).

In lateral and ventral views, the anterior portion of the tongue pad rolled ventrally as the tongue was extended due to the connection to the lower jaw (Figure 3D). Manipulation with forceps showed that the tongue pad was soft and fleshy and did

10974687, 2026, 12, Downloaded from https://onlinelibrary.wiley.com/doi/10.1002/jmor.70195 by Yucheol Shin - American Museum Of Natural , Wiley Online Library on [25/11/2026]. See the Terms and Conditions (https://onlinelibrary.wiley.com/terms-and-conditions) on Wiley Online Library for rules of use; OA articles are governed by the applicable Creative Commons License

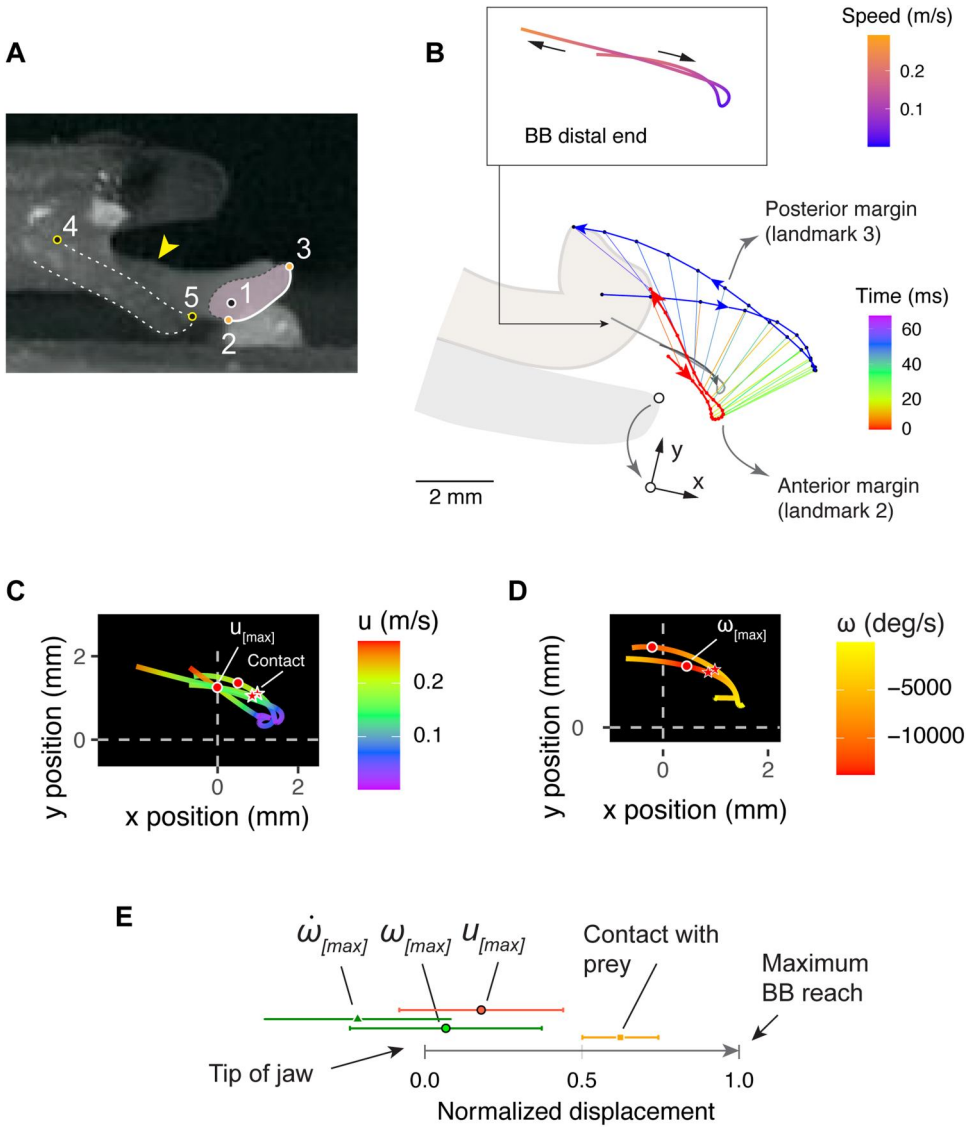


FIGURE 2 | Kinematics of tongue protrusion and tongue pad rotation. (A) Landmarks for motion reconstruction. (B) Trajectories of the anterior edge of tongue pad (red), and the posterior edge of the tongue pad (blue). Line segments represent the orientation of the tongue pad surface, with color representing time. Inset shows the trajectory of the distal end of basibranchial (BB), with color representing speed. (C) Trajectories of the distal end of BB of full protrusion-retraction cycle. Colors represent linear speed. (D) Trajectories of the distal end of BB during protrusion phase. Colors represent tongue pad rotation speed. In (C) and (D), red dots represent peak speeds, and stars represent tongue pad contacting with prey. (E) Spatial locations of the peak linear speed of the distal end of BB ($u_{[max]}$), peak angular acceleration ($\dot{\omega}_{[max]}$) and angular speed ($\omega_{[max]}$) of tongue pad, and the initial contact with prey. Values are mean ± S.D. ($N = 2$ trials, from individuals No. 2 and No. 8). The locations are normalized by the maximum extension of the distal end of BB.

not retain the V-shaped configuration observed in the high-speed videos (Movie 3).

We conducted preliminary examination of the mechanical properties of the hyobranchial skeleton by manually manipulating an isolated specimen in relaxed state. When the hyobranchial skeleton was folded by compressing the EB-CB joints with forceps, it resisted deformation from its resting configuration and tended to recover its original shape after release (Movie 4).

The configuration of the folded hyobranchial skeleton was examined in isolated tongue stalks in a fully protruded state. In dorsal view, the entire structure had a broad base supported by a pair of epibranchials (EB) approximately half the width of the mandible. Compared with the more compact, cylindrical tongue stalk of ballistic-tongued species (e.g., *Eurycea*; see Lombard and Wake 1977), the hyobranchial skeleton of *Karsenia* formed a substantially broader configuration. A large gap was present between the second ceratobranchial (CB2) cartilages, which diverged at an angle of approximately 37° (Figure 4A).

In lateral view, the CB2-BB joint projected dorsally, with an angle of approximately 20° between the longitudinal axes of the two cartilages. This dorsal projection appeared to result from compression at the CB2-BB joint, which bent the enlarged posterior-most region of the BB dorsally (Figure 4B). This elevated joint was also visible in the high-speed video frames (arrowhead in Figure 2A). The glossal ligaments (GL) were

10974687, 2026, 12, Downloaded from https://onlinelibrary.wiley.com/doi/10.1002/jmor.70195 by Yucheol Shin - American Museum Of Natural , Wiley Online Library on [25/11/2026]. See the Terms and Conditions (https://onlinelibrary.wiley.com/terms-and-conditions) on Wiley Online Library for rules of use; OA articles are governed by the applicable Creative Commons License

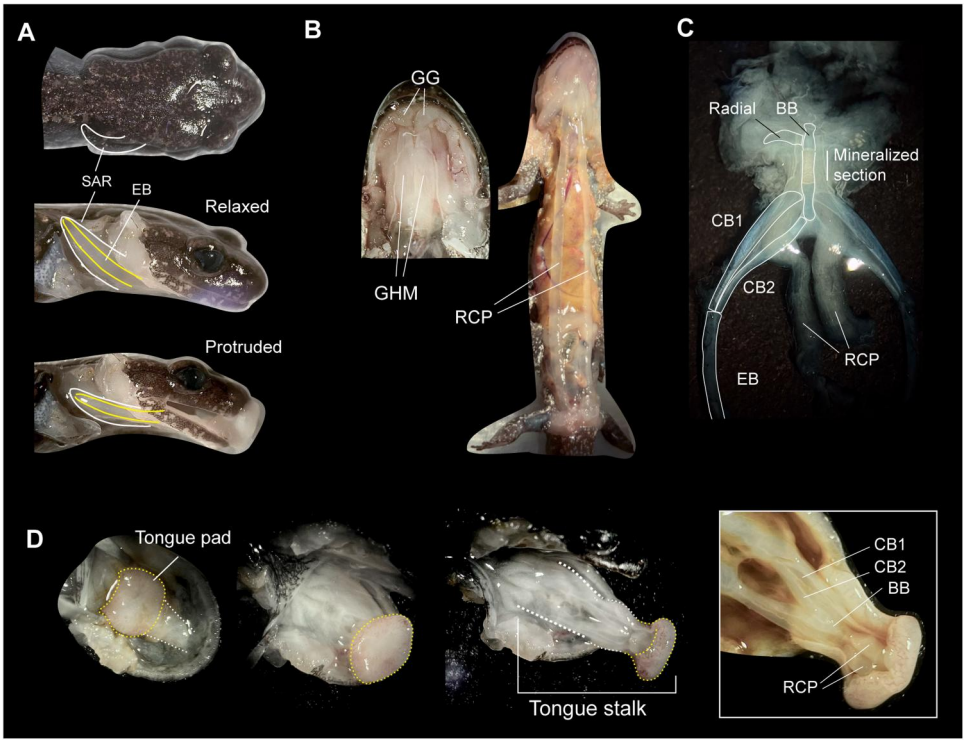


FIGURE 3 | Hyobranchial system of *Karsenia*. (A) Subarcualis rectus (SAR) muscles and epibranchial cartilage (EB) in dorsal and lateral views. (B) Genioglossus (GG), geniohyoideus medialis (GHM), and rectus cervicis profundus (RCP) muscles. (C) Main components of the hyobranchial skeleton, including the basibranchial (BB), first and second ceratobranchial (CB1 and CB2), radial and EB cartilages. In the two dissected individuals, BB length averaged 2.9 ± 0.06 mm (mean ± SD), equivalent to 6.4% ± 0.6% of SVL. (D) Tongue pad (outlined with yellow dashed lines) from resting to fully protruded positions. Inset shows inverted tongue pad in dorsal view. RCP muscles were removed to reveal the skeletal configuration. (A) and (C), individual No. 5; (B) and (D), individual No. 7.

visible as white, taut structures extending from the anterior ends of the first ceratobranchial cartilages (CB1), along the lateral and ventral surfaces of the BB, to its anterodorsal region (Figure 4C–D). In ventral view, the anterior end of each CB1 was articulated with the posterolateral side of the mineralized region of the BB (Figure 4E).

3.4 | Placement of *Karsenia* Within Plethodontid Tongue Diversity

Compared with other plethodontids, *Karsenia* exhibited both low tongue protrusion speed and short relative reach (10% ± 2% SVL; N = 2, one from each of No. 2 and No. 8), placing it near the lower end of the plethodontid performance spectrum. In all protrusive-tongued species, tongue reach did not exceed approximately 10.2% of SVL. Although some protrusive-tongued species had a greater absolute reach than some ballistic-tongued species (including juvenile *Bolitoglossa*), as in *Plethodon* vs. *Hemidactylium* (Figure 5A), the two groups remained clearly differentiated by launch speed (Figure 5B).

Mapping tongue mechanisms onto a recent phylogeny reconstructed two independent origins of ballistic projection within Plethodontidae: one within Plethodontinae at the common ancestor of *Hydromantes* and *Ensatina*, and the other at the common ancestor of Hemidactyliinae (Figure 6A). The two Old World plethodontid lineages (*Karsenia* and *Speleomantes*) occupy opposite regions of the family-wide performance spectrum. *Karsenia* retained a short-reach, slow protrusive mechanism close to the inferred ancestral condition, whereas *Speleomantes* exhibited an extreme ballistic mechanism characterized by long reach and high projection speed. Thus, the surviving Eurasian plethodontids preserve markedly divergent tongue mechanisms despite their shared status as geographically relict lineages (Figure 6B).

4 | Discussion

Our finding that *Karsenia* uses a protrusive tongue is consistent with its retention of several morphological features inferred to represent the ancestral condition in plethodontids (Buckley et al. 2010). Its feeding behavior was generally similar to that of protrusive-tongued salamanders in other families (Larsen and Guthrie 1975; Miller and Larsen 1990; Findeis and Bemis 1990; Reilly and Lauder 1989). However, we did not observe the forward body lunge commonly associated with prey capture in *Plethodon*, *Desmognathus*, and *Aneides* (Larsen and Beneski 1988). Whether this difference represents a species-specific behavior or reflects the restricted experimental conditions remains unclear.

4.1 | Mechanism of the Protrusive Tongue

Tongue protrusion in *Karsenia* appears to be powered directly by contraction of the SAR muscles. The short reach and low protrusion speed place *Karsenia* near the lower end of the performance range among plethodontids. This low-speed mechanism may nevertheless be adequate for capturing prey

10974687, 2026, 12, Downloaded from https://onlinelibrary.wiley.com/doi/10.1002/jmor.70195 by Yucheol Shin - American Museum Of Natural , Wiley Online Library on [25/11/2026]. See the Terms and Conditions (https://onlinelibrary.wiley.com/terms-and-conditions) on Wiley Online Library for rules of use; OA articles are governed by the applicable Creative Commons License

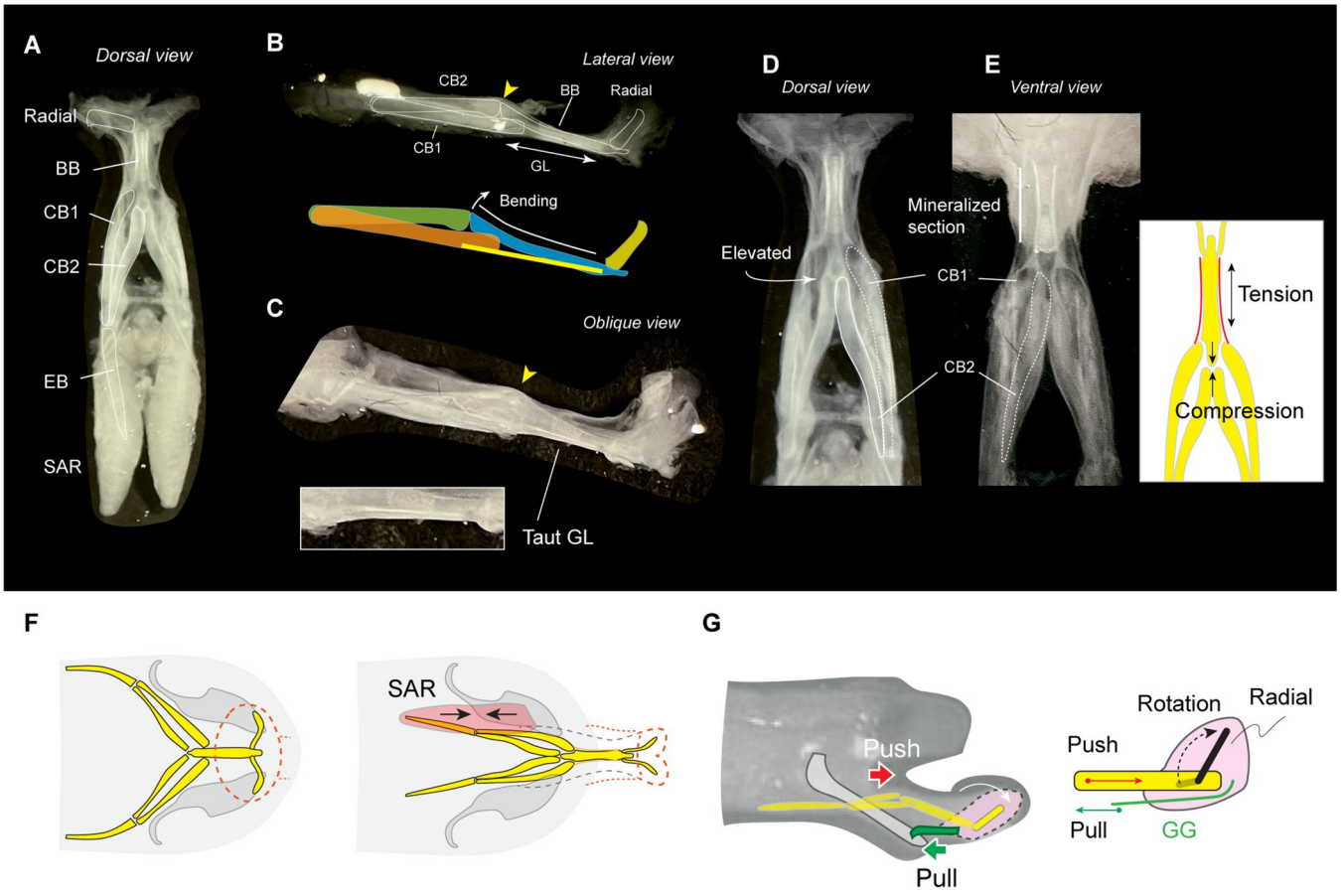


FIGURE 4 | Reconfiguration of hyobranchial skeleton in protruded tongue. (A) Isolated tongue stalk in protruded configuration. (B) Tongue stalk in lateral view, highlighting the elevated CB2-BB joint (yellow arrowhead). (C) Tongue stalk in oblique view, with inset showing the taut glossal ligaments (GL). (D–E) Details of the configuration of CB1-BB and CB2-BB joints. Note the enlarged, posterior-most region of BB is only visible in dorsal view. Inset, schematics of compression at CB2-BB joint and tension on glossal ligaments. (F) Schematics of the reconfiguration of hyobranchial skeleton during tongue protrusion, with tongue pad outlined in dashed lines. (G) Schematic of the mechanism of tongue pad rotation. (A–E), individual No. 7.

at close range within its substrate crevice microhabitats (e.g., under rock piles, fallen logs, and leaf litter) or occasionally on open surfaces during rainy season. However, the ecological significance of its limited reach and speed remains to be tested directly.

The high initial velocity observed at the beginning of the tracked sequence suggests that tongue movement began before or during mouth opening. Consequently, the present recordings probably did not capture the complete acceleration phase. Direct measurements of the onset of SAR shortening and the mass of the active musculature will be required to quantify muscular power output.

An important feature of feeding in *Karsenia* was the forward rotation and transient reconfiguration of the tongue pad. Tongue pad rotation mechanism has received relatively little attention in studies of salamander feeding, although reorientation of the dorsal adhesive surface is necessary for effective contact with prey. As shown in *Karsenia*, several mechanisms may contribute to this reorientation. First, the reconfiguration of the folded hyobranchial skeleton can rotate the basibranchial ventrally by a limited degree (Figure 3F). Second, tightening of the glossal ligaments during skeletal folding may transmit a pulling force to the radial cartilages and tongue pad (see also Lombard and Wake 1977).

In *Karsenia*, the V-shaped configuration of the tongue pad differed from the sac-like or bulbous tongue pad described in other salamanders (Miller and Larsen 1990; Larsen et al. 1996). Because the V shape was apparent during feeding but was not retained during manual manipulation, it appears to be a transient configuration generated dynamically during protrusion. The anteriorly rotated radial cartilages may provide internal support for this shape. The two sides of the tongue pad could therefore increase capture success not only through adhesion but also through partial enclosure of the prey. Whether this configuration produces an active pinching force requires further study across protrusive-tongued plethodontids and direct measurement of interaction forces during tongue-prey contact.

4.2 | Skeletal Folding and Tongue Pad Rotation

Forward translation and tongue pad rotation occurred over similar portions of the protrusion sequence (Figure 2E),

10974687, 2026, 12, Downloaded from https://onlinelibrary.wiley.com/doi/10.1002/jmor.70195 by Yucheol Shin - American Museum Of Natural , Wiley Online Library on [25/11/2026]. See the Terms and Conditions (https://onlinelibrary.wiley.com/terms-and-conditions) on Wiley Online Library for rules of use; OA articles are governed by the applicable Creative Commons License

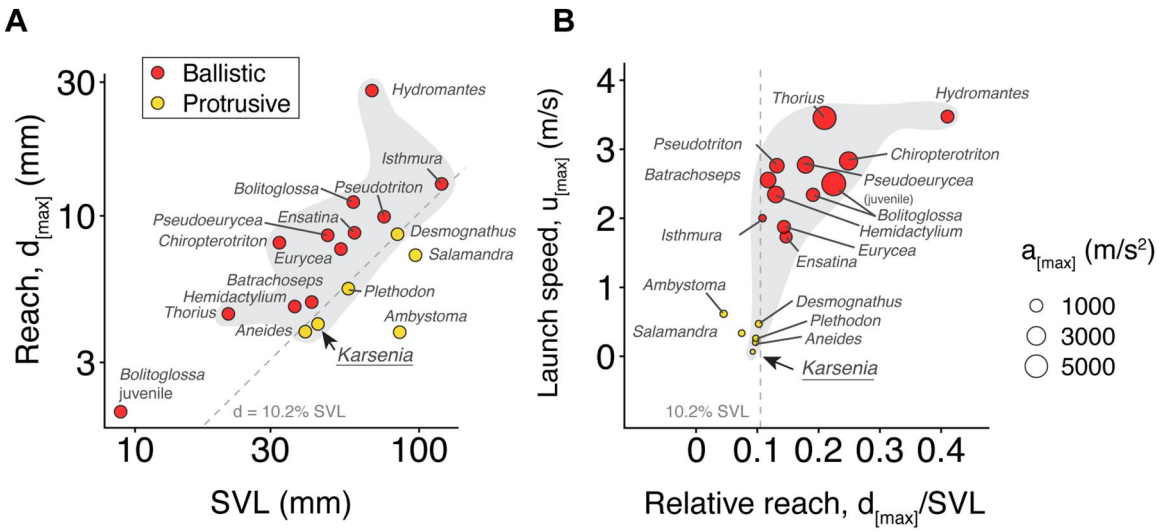


FIGURE 5 | Comparison of tongue feeding capabilities between salamanders. (A) Tongue reach versus SVL. (B) Mean launch speed versus relative reach, with dot size representing the mass-specific power for projection. Values are genus-specific means (data source, Zeng et al. 2025). For *Karsenia*, the mass-specific power ($u_{[max]} \cdot a \sim 3.9$ W/kg) was approximated based on an acceleration time of 10 ms (same time scale of protrusion) and an acceleration $a \approx 19$ m/s^2. Dashed lines represent a threshold of reach ($d_{[max]} \approx 10.2\%SVL$), which separates protrusive and ballistic tongues. Shades highlight values from adult plethodontids.

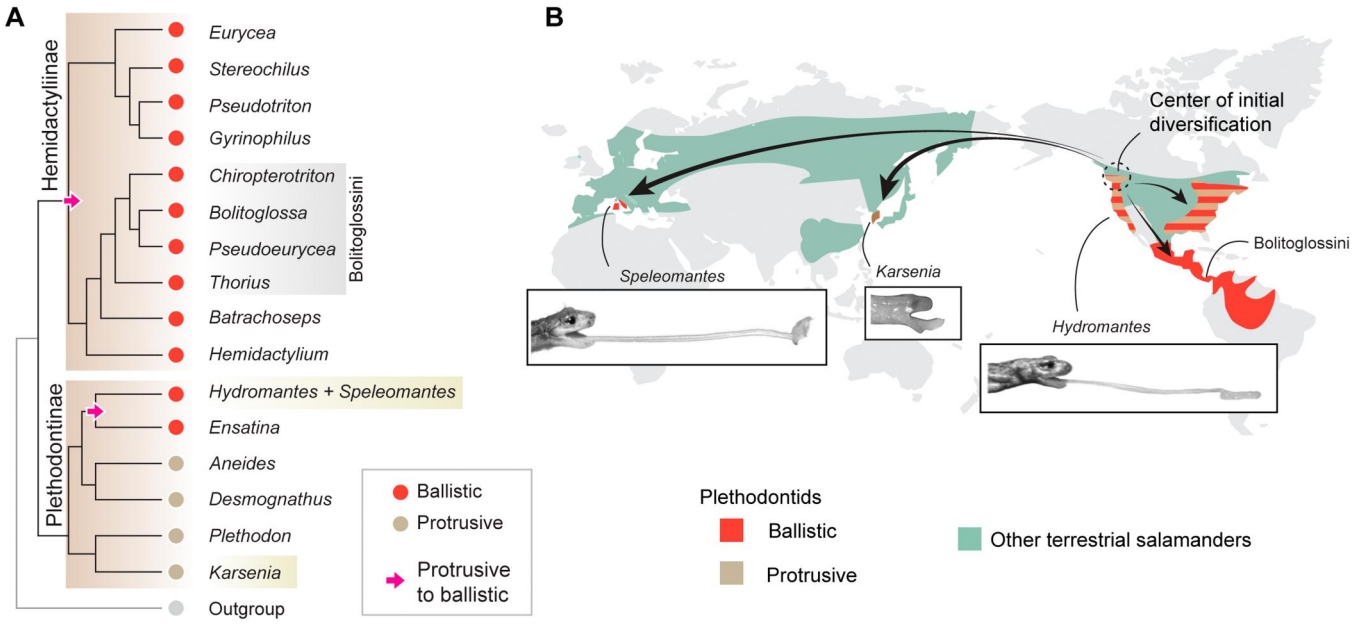


FIGURE 6 | Phylogenetics and global distribution of tongue capability in plethodontids. (A) Phylogenetic mapping of plethodontid tongue mechanism (Deban et al. 2020; Stewart and Wiens 2025). (B) Global distribution of tongue mechanism of plethodontid salamanders. Blue shade shows the schematic distribution of other terrestrial salamanders.

suggesting that the two motions were mechanically coupled. The glossal ligaments provide one possible pathway for this coupling by transmitting reconfiguration of the hyobranchial skeleton (CB1 in particular) to the tongue pad. The presence of glossal ligaments has been confirmed in all other plethodontids (Lombard and Wake 1977), indicating that ligament-mediated pad reorientation may represent an ancestral component of the hyobranchial apparatus in plethodontids. The ventral rolling of the tongue pad tissue is a pulley-like action mediated by the connection to the lower jaw and caused by the forward displacement of the BB. In addition, tightening of the glossal ligaments during skeletal folding may drive rotation of the radial cartilages (Figure 4F–G).

Our observation suggests that the folded hyobranchial skeleton is mechanically unstable and restores to its original geometry, and such elastically influenced behavior may assist in tongue retraction. Several skeletal and ligamentous elements likely contribute to this resistance: (1) bending of the basibranchial (BB), potentially reinforced by its ossified midsection; (2) posterior rotation of the first ceratobranchials (CB1), which increased tension transmitted through the glossal ligaments;

10974687, 2026, 12, Downloaded from https://onlinelibrary.wiley.com/doi/10.1002/jmor.70195 by Yucheol Shin - American Museum Of Natural , Wiley Online Library on [25/11/2026]. See the Terms and Conditions (https://onlinelibrary.wiley.com/terms-and-conditions) on Wiley Online Library for rules of use; OA articles are governed by the applicable Creative Commons License

and (3) deformation associated with the dorsally elevated CB2-BB joints (Figure 4B). This proposed mechanism requires confirmation through measurements of deformation, restoring forces, and energy storage and release of skeletal and tissue elements during tongue protrusion and retraction.

Future studies should examine the mechanisms of tongue pad reorientation across protrusive-tongued plethodontids. Potential contributors include SAR-driven protrusion, reconfiguration of the hyobranchial skeleton, tension in the glossal ligaments, and the tissue connection between the tongue pad to the lower jaw, especially the activity of the genioglossus muscles after tongue tip protrudes beyond the margin of the lower jaw. Comparative analyses should also test how tongue kinematics scale with body size. Finally, variation in skeletal folding configuration, from partial folding in *Karsenia* to the more compactly folded skeleton (such as *Hydromantes*), may help reveal the structural optimization toward ballistic projectile tongues.

4.3 | Implications for *Karsenia* Ecology

As salamander feeding behavior may depend on prey type and size (Deban and Bloom 2018), therefore the use of a single prey type in the present study has limitations. The short tongue reach observed in *Karsenia* is consistent with a diet dominated by ants and other small invertebrates (Ju 2009), which may often be encountered at close range within their microhabitats. During our feeding trials, *Karsenia* oriented themselves toward visually conspicuous prey, suggesting that visual cues can contribute to prey detection under laboratory conditions. However, the relative importance of visual, chemical, and tactile cues under natural conditions remains unknown.

Based on previous observations of its natural history and activity patterns, *Karsenia* becomes more active during the rainy season and may either actively search for prey or capture invertebrates encountered within crevices (Song et al. 2017; Jung et al. 2019). These behaviors may resemble those of North American plethodontines such as *Plethodon* and *Aneides*, although the small body size and the dependence on substrate-crevice microhabitats of *Karsenia* may constrain its movement and foraging range.

Further field observations are needed to characterize prey-detection mechanisms, foraging mode, and feeding performance under natural conditions. Quantifying the spatial structure, prey availability, and light environment of microhabitats would also help determine the functionality of the short-reach protrusive tongue in *Karsenia*.

4.4 | History of Old-World Plethodontids

The contrasting tongue mechanisms of *Karsenia* and *Speleomantes* suggest that feeding capability alone does not explain the present distribution of plethodontids in Eurasia. Their restricted modern distribution is consistent with the result of ancient transcontinental dispersal followed by massive, climate-driven extinction. Plethodontids dispersed into Eurasia during the Late Cretaceous, but their range subsequently contracted as climates cooled and became drier after the Eocene (Vieites et al. 2007; Wake 2009, 2013; Shen et al. 2016).

The wide geographic separation between *Karsenia* and *Speleomantes* implies the historical loss of lineages that were likely distributed across Eurasia, although their taxonomic and functional diversity remains unknown. Because lungless salamanders rely heavily on cutaneous respiration, their activity, dispersal, and persistence are strongly constrained by temperature and moisture. Long-term cooling, drying, and fragmentation of humid habitats may therefore have reduced connectivity across northern Eurasia and eliminated intervening lineages.

The survival of *Karsenia* and *Speleomantes* may thus reflect historical and geographic contingency. Rocky, humid, and thermally buffered habitats, including talus slopes within well-shaded forests and karstic cave systems, may have served as refugia for both lineages. The woodlands with metamorphic rocks of the Korean Peninsula and the rocky subterranean habitats of the Mediterranean provide cool, moist microhabitats that can buffer salamanders from external variation in temperature and moisture (Jeon et al. 2021; Salvidio et al. 2025). These environmental conditions may have allowed the two lineages to persist despite extensive climatic and geographic change elsewhere in Eurasia.

Other Eurasian salamander families (e.g., Salamandridae) occupy broader geographic and ecological ranges, potentially reflecting differences in respiratory biology, life history, dispersal ability, and habitat use. The survival of plethodontid lineages at opposite ends of the tongue capability spectrum nevertheless suggests that their persistence was probably shaped more strongly by historical biogeography and refugial habitat availability than by a particular feeding specialization.

5 | Conclusion

Our study provides the first integrated description of feeding behavior, tongue kinematics, and hyobranchial morphology in *Karsenia koreana*. *Karsenia* uses a short-reach, muscle-powered protrusive tongue characterized by low projection speed, limited reach, and coordinated rotation and transient reconfiguration of the tongue pad. Anatomical observations further suggest that tongue pad motion is mechanically coupled with reconfiguration of the hyobranchial skeleton through connections involving the genioglossus muscles, glossal ligaments, and radial cartilages.

These findings place *Karsenia* near the low-performance end of the plethodontid tongue feeding spectrum and are consistent with retention of a protrusive mechanism close to the inferred ancestral condition. In contrast to the highly specialized ballistic tongue of the other surviving Old World lineage, *Speleomantes*, the feeding system of *Karsenia* highlights the substantial functional divergence retained among Eurasian plethodontids. Together, these results fill an important phylogenetic gap and provide a basis for future comparative studies on how anatomical reconfiguration, soft-tissue coupling, and

10974687, 2026, 12, Downloaded from https://onlinelibrary.wiley.com/doi/10.1002/jmor.70195 by Yucheol Shin - American Museum Of Natural , Wiley Online Library on [25/11/2026]. See the Terms and Conditions (https://onlinelibrary.wiley.com/terms-and-conditions) on Wiley Online Library for rules of use; OA articles are governed by the applicable Creative Commons License

skeletal design contributed to the evolution of ballistic tongue projection in Plethodontidae.

Author Contributions

Yu Zeng: conceptualization, investigation, writing – original draft, methodology, validation, visualization, writing – review and editing, software, formal analysis, project administration, data curation, supervision, resources. **Jiho Park:** methodology, investigation, writing – review and editing, project administration, data curation, supervision, resources, validation, conceptualization. **Yucheol Shin:** investigation, methodology, validation, writing – review and editing, project administration, supervision, resources, conceptualization. **Daesik Park:** methodology, validation, writing – review and editing, project administration, supervision, resources, conceptualization. **Stephen M. Deban:** conceptualization, investigation, methodology, writing – review and editing, project administration, supervision, resources.

Acknowledgements

We thank Seo-gu District Office, Daejeon Metropolitan City, South Korea for the collection permit. We thank Jun Kim for assistance in the field and in the laboratory. We are grateful for comments from Anthony Powell and Claire Crookston. Y.S. was supported by the Richard Gilder Graduate School Doctoral Fellowship and RGGS Sydney Anderson Travel Award from the American Museum of Natural History during fieldwork and writing of this manuscript. We dedicate this paper in memory of David B. Wake in recognition of his work on the functional morphology and evolution of the feeding apparatus in plethodontid salamanders.

Data Availability Statement

The data that support the findings of this study are available in the supplementary material of this article. Additional data are available on request from the corresponding author.

Peer Review

For transparency, the peer review documents associated with this article are available at https://doi.org/10.1002/jmor.70195.

References

AmphibiaWeb. 2026. *AmphibiaWeb*. University of California. Accessed September 27, 2026. https://amphibiaweb.org.

Buckley, D., M. H. Wake, and D. B. Wake. 2010. "Comparative Skull Osteology of *Karsenia koreana* (Amphibia, Caudata, Plethodontidae)." *Journal of Morphology* 271: 533–558. https://doi.org/10.1002/jmor.10816.

Deban, S. M., and S. V. Bloom. 2018. "Ballistic Tongue Projection in a Miniaturized Salamander." *Journal of Experimental Zoology Part A: Ecological and Integrative Physiology* 329: 62–71. https://doi.org/10.1002/jez.2171.

Deban, S. M., J. C. O'Reilly, U. Dicke, and J. L. Van Leeuwen. 2007. "Extremely High-Power Tongue Projection in Plethodontid Salamanders." *Journal of Experimental Biology* 210: 655–667. https://doi.org/10.1242/jeb.02664.

Deban, S. M., and J. A. Scales. 2016. "Dynamics and Thermal Sensitivity of Ballistic and Non-Ballistic Feeding in Salamanders." *Journal of experimental biology* 219: 431–444. https://doi.org/10.1242/jeb.127407.

Deban, S. M., J. A. Scales, S. V. Bloom, C. M. Easterling, M. K. O'Donnell, and J. P. Olberding. 2020. "Evolution of a High-Performance and Functionally Robust Musculoskeletal System in Salamanders." *Proceedings of the National Academy of Sciences* 117: 10445–10454. https://doi.org/10.1073/pnas.1921807117.

Deban, S. M., D. B. Wake, and G. Roth. 1997. "Salamander With a Ballistic Tongue." *Nature* 389: 27–28. https://doi.org/10.1038/37898.

Lombard, R., and D. B. Wake. 1977. "Tongue Evolution in the Lungless Salamanders, Family Plethodontidae. II. Function and Evolutionary Diversity." *Journal of Morphology* 153: 39–79. https://doi.org/10.1002/jmor.1051530104.

Findeis, E. K., and W. E. Bemis. 1990. "Functional Morphology of Tongue Projection in *Taricha torosa* (Urodela: Salamandridae)." *Zoological Journal of the Linnean Society* 99: 129–157. https://doi.org/10.1111/j.1096-3642.1990.tb00565.x.

Hedrick, T. L. 2008. "Software Techniques for Two- and Three-Dimensional Kinematic Measurements of Biological and Biomimetic Systems." *Bioinspiration & Biomimetics* 3: 034001. https://doi.org/10.1088/1748-3182/3/3/034001.

Jeon, J. Y., J. Jung, H. Y. Suk, H. Lee, and M.-S. Min. 2021. "The Asian Plethodontid Salamander Preserves Historical Genetic Imprints of Recent Northern Expansion." *Scientific Reports* 11: 9193. https://doi.org/10.1038/s41598-021-88238-z.

Ju, H.-Y. 2009. "Taxonomic Study on Some Anatomical Characters and Prey Resource of the Endemic Species *Karsenia koreana* (Amphibia, Caudata, Plethodontidae) in Korea." Master's thesis, University of Incheon.

Jung, J.-H., E.-J. Lee, W.-S. Lee, and C.-D. Park. 2019. "Habitat Suitability Models of Korean crevice salamander (*Karsenia koreana*) at Forested Area in Daejeon Metropolitan City, Republic of Korea." *Journal of Forest Research* 24: 349–355. https://doi.org/10.1080/13416979.2019.1693479.

Larsen, Jr., J. H., J. T. Beneski, Jr., and B. T. Miller. 1996. "Structure and Function of the Hyolingual System in *Hynobius* and Its Bearing on the Evolution of Prey Capture in Terrestrial Salamanders." *Journal of Morphology* 227: 235–248. https://doi.org/10.1002/(SICI)1097-4687(199602)227:2<235::AID-JMOR9>3.0.CO;2-7.

Larsen, Jr., J. H., and D. J. Guthrie. 1975. "The Feeding System of Terrestrial Tiger Salamanders (*Ambystoma tigrinum melanostictum* Baird)." *Journal of Morphology* 147: 137–153. https://doi.org/10.1002/jmor.1051470203.

Larsen, Jr., J. H., and J. T. Beneski, Jr. 1988. "Quantitative Analysis of Feeding Kinematics in Dusky Salamanders (*Desmognathus*)." *Canadian Journal of Zoology* 66: 1309–1317. https://doi.org/10.1139/z88-192.

Lombard, R. E., and D. B. Wake. 1986. "Tongue Evolution in the Lungless Salamanders, Family Plethodontidae. IV. Phylogeny of Plethodontid Salamanders and the Evolution of Feeding Dynamics." *Systematic Zoology* 35: 532–551. https://doi.org/10.2307/2413113.

Miller, B. T., and J. H. Larsen, Jr. 1990. "Comparative Kinematics of Terrestrial Prey Capture in Salamanders and Newts (Amphibia: Urodela: Salamandridae)." *Journal of Experimental Zoology* 256: 135–153. https://doi.org/10.1002/jez.1402560204.

Min, M.-S., S. Y. Yang, R. M. Bonett, D. R. Vieites, R. A. Brandon, and D. B. Wake. 2005. "Discovery of the First Asian Plethodontid Salamander." *Nature* 435: 87–90. https://doi.org/10.1038/nature03474.

R Core Team. 2023. R: A Language and Environment for Statistical Computing. R Foundation for Statistical Computing.

Reilly, S. M., and G. V. Lauder. 1989. "Kinetics of Tongue Projection in *Ambystoma tigrinum*: Quantitative Kinematics, Muscle Function, and Evolutionary Hypotheses." *Journal of Morphology* 199: 223–243. https://doi.org/10.1002/jmor.1051990208.

Rueden, C. T., J. Schindelin, M. C. Hiner, et al. 2017. "ImageJ2: Imagej for the Next Generation of Scientific Image Data." *BMC Bioinformatics* 18: 529. https://doi.org/10.1186/s12859-017-1934-z.

Salvidio, S., A. Costa, F. Oneto, G. Rosa, and M. V. Pastorino. 2025. "No Change over Three Decades in the Realized Spatial Niche of a Salamander Population Living in a Subterranean Habitat." *Current Zoology* 71: 678–681. https://doi.org/10.1093/cz/zoaf016.

Shen, X.-X., D. Liang, M.-Y. Chen, R.-L. Mao, D. B. Wake, and P. Zhang. 2016. "Enlarged Multilocus Data Set Provides Surprisingly Younger Time of Origin for the Plethodontidae, the Largest Family of

10974687, 2026, 12, Downloaded from https://onlinelibrary.wiley.com/doi/10.1002/jmor.70195 by Yucheol Shin - American Museum Of Natural , Wiley Online Library on [25/11/2026]. See the Terms and Conditions (https://onlinelibrary.wiley.com/terms-and-conditions) on Wiley Online Library for rules of use; OA articles are governed by the applicable Creative Commons License

Salamanders." *Systematic Biology* 65: 66–81. https://doi.org/10.1093/sysbio/syv061.

Song, J.-Y., M. Matsui, T. Matsuki, K. Nishikawa, K.-S. Koo, and H.-S. Oh. 2017. "Life History of a Unique Asian Plethodontid Salamander, *Karsenia koreana*." *Zoological Science* 34: 122–128. https://doi.org/10.2108/zs160158.

Stewart, A. A., and J. J. Wiens. 2025. "A Time-Calibrated Salamander Phylogeny Including 765 Species and 503 Genes." *Molecular Phylogenetics and Evolution* 204: 108272. https://doi.org/10.1016/j.ympev.2024.108272.

Vieites, D. R., M.-S. Min, and D. B. Wake. 2007. "Rapid Diversification and Dispersal During Periods of Global Warming by Plethodontid Salamanders." *Proceedings of the National Academy of Sciences* 104: 19903–19907. https://doi.org/10.1073/pnas.0705056104.

Wake, D. B. 1991. "Homoplasy: The Result of Natural Selection, or Evidence of Design Limitations?" *American Naturalist* 138: 543–567. https://doi.org/10.1086/285234.

Wake, D. B. 2009. "What Salamanders Have Taught Us about Evolution." *Annual Review of Ecology, Evolution, and Systematics* 40: 333–352. https://doi.org/10.1146/annurev.ecolsys.39.110707.173552.

Wake, D. B. 2013. "The Enigmatic History of the European, Asian, and American Plethodontid Salamanders." *Amphibia-Reptilia* 34: 323–336. https://doi.org/10.1163/15685381-00002893.

Wake, D. B., and S. M. Deban. 2000. "Terrestrial Feeding in Salamanders." In *Feeding: Form, Function and Evolution in Tetrapod Vertebrates*, edited by In. K. Schwenk, 95–116. Academic Press.

Zeng, Y., C. V. Anderson, and S. M. Deban. 2025. "Convergently Evolved Linear Actuators in Ballistic Tongues." *Current Biology* 35: 4229–4240.e5. https://doi.org/10.1016/j.cub.2025.07.085.

Zeng, Y., and S. M. Deban. 2026. "Ballistic Tongues." *Current Biology* 36: R426–R427. https://doi.org/10.1016/j.cub.2026.03.051.

Supporting Information

Additional supporting information can be found online in the Supporting Information section.

Data S1: Body size and mass of collected specimens.

Movie S2: Full feeding sequence of *Karsenia* (replayed ~6.6 times slower than the actual speed; individual No. 8).

Movie S3: Tongue feeding of *Karsenia* in lateral view (replayed ~33 times slower than the actual speed; individual No. 8).

Movie S4: Manipulating tongue pad with forceps.

Movie S5: Manually folding the hyobranchial skeleton by compressing the EB-CB joints with forceps.

10974687, 2026, 12, Downloaded from https://onlinelibrary.wiley.com/doi/10.1002/jmor.70195 by Yucheol Shin - American Museum Of Natural , Wiley Online Library on [25/11/2026]. See the Terms and Conditions (https://onlinelibrary.wiley.com/terms-and-conditions) on Wiley Online Library for rules of use; OA articles are governed by the applicable Creative Commons License